Modeling Effects of Oxyanion Hole on the Ester Hydrolysis Catalyzed by Human Cholinesterases

Daquan Gao and Chang-Guo Zhan*

Department of Pharmaceutical Sciences, College of Pharmacy, University of Kentucky, 725 Rose Street, Lexington, Kentucky 40536

Received: July 7, 2005; In Final Form: September 18, 2005

Molecular dynamics (MD) simulations and hydrogen bonding energy (HBE) calculations have been performed on the prereactive enzyme−substrate complexes (ES), transition states (TS1), and intermediates (INT1) for acetylcholinesterase (AChE)-catalyzed hydrolysis of acetylcholine (ACh), butyrylcholinesterase (BChE)-catalyzed hydrolysis of ACh, and BChE-catalyzed hydrolysis of (+)/(−)-cocaine to examine the protein environmental effects on the catalytic reactions. The hydrogen bonding of cocaine with the oxyanion hole of BChE is found to be remarkably different from that of ACh with AChE/BChE. Whereas G121/G116, G122/G117, and A204/A199 of AChE/BChE all can form hydrogen bonds with ACh to stabilize the transition state during the ACh hydrolysis, BChE only uses G117 and A199 to form hydrogen bonds with cocaine. The change of the estimated total HBE from ES to TS1 is ca. −5.4/-4.4 kcal/mol for AChE/BChE-catalyzed hydrolysis of ACh and ca. −1.7/−0.8 kcal/mol for BChE-catalyzed hydrolysis of (+)/(−)-cocaine. The remarkable difference of ∼3 to 5 kcal/mol reveals that the oxyanion hole of AChE/BChE can lower the energy barrier of the ACh hydrolysis significantly more than that of BChE for the cocaine hydrolysis. These results help to understand why the catalytic activity of AChE against ACh is considerably higher than that of BChE against cocaine and provides valuable clues on how to improve the catalytic activity of BChE against cocaine.

Introduction

Cholinesterases, including both acetylcholinesterase (AChE) and butyrylcholinesterase (BChE), are serine hydrolases that have important roles in cholinergic neurotransmission and are involved in other nervous system functions and in neurodegenerative diseases.[1,2] These enzymes can catalyze hydrolysis of neurotransmitter acetylcholine (ACh) and related carboxylic acid esters. Both AChE and BChE are important targets for the development of cholinergic drugs.[3−6] BChE is also the primary cocaine-metabolizing enzyme in the plasma. BChE can catalyze hydrolysis of cocaine at the benzoyl ester group.[6]

Cocaine addiction and overdose are a major medical and public health problem that continues to defy treatment.[7,8] The disastrous medical and social consequences of cocaine addiction, such as violent crime, loss in individual productivity, illness, and death, have made the development of an effective pharmacological treatment a high priority.[9,10] However, cocaine mediates its reinforcing and toxic effects by blocking neurotransmitter reuptake and the classical pharmacodynamic approach has failed to yield small-molecule receptor antagonists due to the difficulties inherent in blocking a blocker.[7−10] An alternative to receptor-based approaches is to interfere with the delivery of cocaine to its receptors and accelerate its metabolism in the body.[10] Extensive experimental studies in animals and humans demonstrate that enhancement of BChE activity by administration of exogenous enzyme substantially decreases cocaine half-life.[11−14] So, enhancement of cocaine metabolism by administration of BChE has been recognized to be a promising pharmacokinetic approach for treatment of cocaine abuse and dependence.[10] However, the catalytic activity of this plasma enzyme is relatively low against cocaine.[15,16] BChE-catalyzed hydrolysis of cocaine is considerably slower than AChE-catalyzed hydrolysis of ACh. Hence, BChE mutants with a higher activity against cocaine are highly desirable for therapeutic use in humans.

It is crucial for rational design of high-activity BChE mutants against cocaine to know the detailed reaction mechanism concerning how cocaine is hydrolyzed by human BChE and to understand the mechanistic difference between BChE-catalyzed hydrolysis of cocaine and AChE-catalyzed hydrolysis of ACh. Extensive experimental and computational studies have been reported on the reaction mechanism for AChE-catalyzed hydrolysis of ACh.[17−31] Most of the computational studies of the reaction coordinate have focused on the initial step of the acylation,[27] because this reaction step is the rate-determining step of the chemical process. The computational studies demonstrate how the protein environment can stabilize the transition state structure and, therefore, lower the energy barrier for this key reaction step of AChE-catalyzed hydrolysis of ACh. Computational studies on BChE−cocaine complex led to the understanding of how cocaine binds with BChE.[32−36] Ab initio reaction coordinate calculations were also performed on a simplified BChE active site model neglecting the protein environmental effects.[35] The reaction coordinate calculations demonstrated that the fundamental reaction pathway for BChE-catalyzed hydrolysis of cocaine should be similar to that for AChE-catalyzed hydrolysis of ACh in terms of the breaking and formation of covalent bonds during the catalytic hydrolysis, as shown in Figure 1.[35,36] In particular, residues S198, H438, and E325 of BChE clearly form a catalytic triad, corresponding to the well-known catalytic triad consisting of S203, H447, and

* Address correspondence to this author. Phone: 859-323-3943. Fax: 859-323-3575. E-mail: zhan@uky.edu.

10.1021/jp053736x CCC: $30.25
Published on Web 11/08/2005

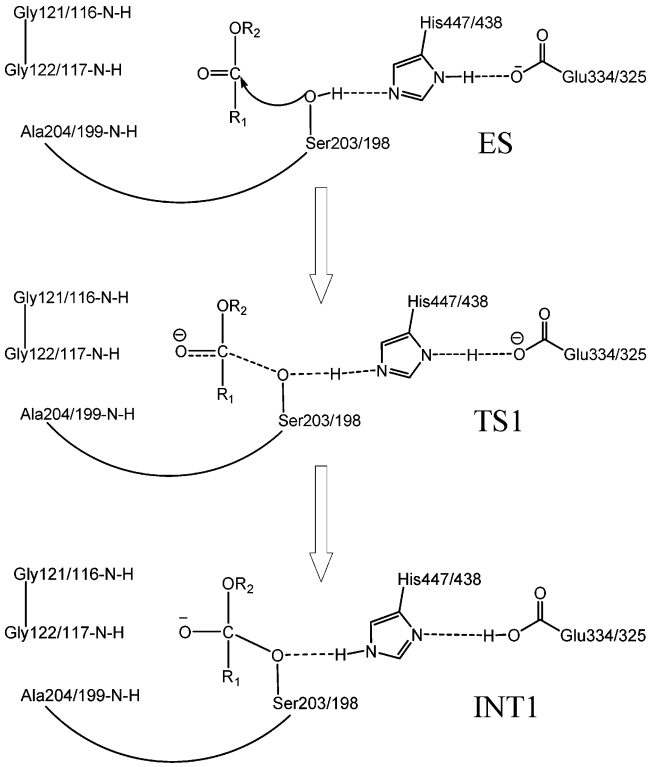

Figure 1. Schematic representation of the common pathway for the initial reaction step of AChE/BChE-catalyzed hydrolysis of ACh/cocaine.

E334 of AChE. In addition, the MD simulations of the prereactive BChE−cocaine complex[35,36] also led to a mechanistic hypothesis that the peptidic NH groups of G116, G117, and A199 could constitute a possible oxyanion hole forming up to three strong N−H···O hydrogen bonds with the negatively charged carbonyl oxygen of the benzoyl ester group of cocaine in the transition state and intermediate. This putative three-pronged oxyanion hole of BChE, if indeed it exists, would be similar to the well-known three-pronged oxyanion hole formed from G121, G122, and A204 of AChE.[27] However, it is unclear whether the possible N−H···O hydrogen bonding between the oxyanion hole of the enzyme and the carbonyl oxygen of substrate is affected differently by the different protein environments in AChE and BChE.

Here we report a computational study using a new computational strategy to evaluate the protein environmental effects on the possible N−H···O hydrogen bonds between the oxyanion hole of the enzyme and the carbonyl oxygen of substrate for AChE-catalyzed hydrolysis of ACh, BChE-catalyzed hydrolysis of (+)-cocaine, and BChE-catalyzed hydrolysis of (−)-cocaine. For comparison, BChE-catalyzed hydrolysis of ACh was also examined. The new strategy starts from molecular dynamics (MD) simulations on the prereactive enzyme−substrate complex (ES), first transition state (TS1), and first intermediate (INT1), followed by a theoretical estimation of the hydrogen bonding energy (HBE) of the substrate with the oxyanion hole for each simulated structure in water. The MD simulations and HBE calculations allow us to reveal, for the first time, the possible differences between these enzymatic reactions concerning the protein environmental effects and their roles in stabilizing the transition states and lowering the energy barriers. The results obtained from the comparative study of these enzymatic reactions provide valuable clues on how to improve the catalytic activity of BChE against cocaine through rational design of site-directed mutagenesis.

Computational Methods

The starting three-dimensional (3D) structure of human AChE used in the MD simulations was from the X-ray crystal structure[37] deposited in the Protein Data Bank (PDB access code 1B41).[38] The starting 3D structure of human BChE was from the X-ray crystal structure (pdb code 1P0P).[39] The missing residues (D2, D3, E255, D378, D379, N455, L530, E531, and M532) in the X-ray crystal structure of BChE were built by the automated homology modeling tool Modeler[40,41]/InsightII software (Accelrys, Inc.) with the default parameters. The initial geometries of the prereactive enzyme−substrate (ES) complexes were constructed from the previous MD simulations on the prereactive BChE−cocaine complexes based on a homology model.[35]

We must address a critical issue before describing how we performed any MD simulation on a transition state. In principle, MD simulation using a classical force field (molecular mechanics) can only simulate a stable structure corresponding to a local minimum on the potential energy surface, whereas a transition state during a reaction process is always associated with a first-order saddle point on the potential energy surface. Hence, MD simulation using a classical force field cannot directly simulate a transition state without any restraint on the geometry of the transition state. Nevertheless, if we can technically remove the freedom of imaginary vibration in the transition state structure, then the number of vibrational freedoms (normal vibration modes) for a nonlinear molecule will decrease from $3N - 6$. The transition state structure is associated with a local minimum on the potential energy surface within a subspace of the reduced vibrational freedoms, although it is associated with a first-order saddle point on the potential energy surface with all of the $3N - 6$ vibrational freedoms. Theoretically, the vibrational freedom associated with the imaginary vibrational frequency in the transition state structure can be removed by appropriately freezing the reaction coordinate. The reaction coordinate corresponding to the imaginary vibration of the transition state is generally characterized by a combination of some key geometric parameters. These key geometric parameters are bond lengths of the forming and breaking covalent bonds for BChE-catalyzed hydrolysis of cocaine, as seen in Figure 1. Thus, we just need to maintain the bond lengths of the forming and breaking covalent bonds during the MD simulation on each transition state. Technically, we can maintain the bond lengths of the forming and breaking covalent bonds by simply fixing all atoms within the reaction center, by using some constraints on the forming and breaking covalent bonds, or by redefining the forming and breaking covalent bonds. It should be pointed out that the only purpose of performing this type of MD simulation on a transition state is to examine the dynamic change of the protein environment surrounding the reaction center and the interaction between the reaction center and the protein environment. We are only interested in the simulated structures, as the total energies calculated in this way are meaningless.

We note that S203/S198 in the catalytic triad of AChE/BChE is no longer a standard residue in the transition states and intermediates. For each transition state or intermediate, the fundamental structure of the reaction center was maintained by redefining the covalent bonds that will break or form during the reaction process. Such a covalent bond is only partially formed or partially broken in a transition state. This type of partial covalent bond in TS1 may be called a "transition" covalent bond. For convenience, each of the transition covalent bonds was technically defined as a "formal" covalent bond whose standard bond length (r_0) was the same as the corre-

sponding internuclear distance optimized by the ab initio reaction coordinate calculations on the simplified model systems;[35] the same level of first-principles reaction coordinate calculation was also performed for the model system of AChE/BChE-catalyzed hydrolysis of ACh (unpublished data). Thus, in the TS1 structure, there exists a formal covalent bond between H447/H438 and E334/E325 and a formal covalent bond between S203/S198 and H447/H438, although H447/H438 and E334/E325 were still regarded as the standard residues in terms of the used force field parameters and partial atomic charges. The dash lines in the TS1 structure drawn in Figure 1 all represent the transition covalent bonds. There is no transition covalent bond in any of the ES and INT1 structures.

The partial atomic charges for the nonstandard residue atoms, including the substrate atoms, were estimated by using the RESP protocol implemented in the Antechamber module of the Amber7 package[42] following electrostatic potential (ESP) calculations with the Gaussian03 program[43] at the ab initio HF/6-31G* level. Determination of the RESP charges was straightforward for the substrate in the ES structure, as we only needed to calculate the separate substrate structure. The TS1 and INT1 model geometries used in the ESP calculations came from those obtained from the ab initio reaction coordinate calculations on the simplified model systems,[35] but the functional groups representing the oxyanion hole were removed. For all of the substrate atoms in the TS1/INT1 structure, the directly calculated RESP charges were used as the corresponding partial atomic charges, although the total of the RESP charges determined for the substrate atoms is not an integer due to the expected charge transfer between the substrate and S203/S198 during the reaction process. For example, without charge transfer, the total of the RESP charges for the substrate atoms should be +1.000 in the TS1 structure, whereas the actually calculated total of the RESP charges for the (−)-cocaine atoms was +0.670 in the TS1 structure. Therefore, we needed to change the partial atomic charges on some atoms in S203/S198 to obtain the correct total charge of the entire reaction system in the TS1 and INT1 structures. We wanted to minimize the number of atoms whose partial atomic charges must be changed from those in the standard serine residue. Hence, the partial atomic charges in the standard serine residue were used for all atoms in S203/S198, except for the hydroxyl oxygen atom (O^{γ}) whose partial atomic charge was chosen to reflect the charge transfer between the substrate and S203/S198 in the TS1 and INT1 structures.

The initial geometries of the transition states (TS1) and intermediates (INT1) used to perform the MD simulations were based on the TS1 and INT1 geometries obtained from the ab initio reaction coordinate calculations[35] on the corresponding simplified model systems that completely neglect the protein environment effects. Technically, for each TS1/INT1 structure, we started from the final snapshot of the simulated ES structure and performed an energy minimization by using the force field parameters and partial atomic charges determined for the corresponding TS1/INT1 structure. The energy minimization automatically and quickly led to a modified geometry reflecting the essential structural features of the reaction center in the expected TS1/INT1 structure, particularly for the lengths of the defined covalent bonds. Such a modified geometry was used for the equilibration before the MD simulation for each TS1/INT1 structure.

Each aforementioned initial geometry was neutralized by adding chloride counterions and was solvated in a rectangular box of TIP3P water molecules[44] with a minimum solute−wall distance of 10 Å. The general procedure for carrying out the MD simulations in water is essentially the same as that used in our other previously reported computational studies.[35,36,45] The MD simulations in this study were performed by using the Sander module of the Amber7 package. The solvated systems were carefully equilibrated and fully energy minimized. These systems were gradually heated from $T = 10$ to 298.15 K in 30 ps before a long MD simulation at $T = 298.15$ K, making sure that we obtained a stable MD trajectory for each of the simulated structures. The time step used for the MD simulations was 2 fs. Periodic boundary conditions in the NPT ensemble at $T = 298.15$ K with Berendsen temperature coupling[46] and $P = 1$ atm with isotropic molecule-based scaling[46] were applied. The SHAKE algorithm[47] was used to fix all covalent bonds containing hydrogen atoms. The nonbonded pair list was updated every 10 steps. The particle mesh Ewald (PME) method[48] was used to treat long-range electrostatic interactions. A residue-based cutoff of 10 Å was utilized for the Lennard-Jones interactions. The coordinates of the simulated systems were collected every 1 ps during the production MD stages.

Most of the MD simulations were performed on a HP supercomputer at the Center for Computational Sciences, University of Kentucky. The other computations were carried out on an IBM ×335 Linux cluster and SGI Fuel workstations in our own lab.

Results and Discussion

Simulated Structures. The structures of ES, TS1, and INT1 in water were simulated for 500 ps or longer to make sure we obtained a stable MD trajectory for each of the simulated systems. The MD trajectories actually became stable quickly, as were the internuclear distances involved in the potential N−H···O hydrogen bonds, i.e., the distances from the carbonyl oxygen of substrate ACh/cocaine to the NH hydrogen atoms of G121/G116, G122/G117, and A204/A199 of AChE/BChE. Depicted in Figures 2 and 3 are plots of these important distances in the MD-simulated structures versus the simulation time, along with root-mean-square deviation (RMSD) of the positions of backbone atoms in the simulated structures from those in the corresponding initial structures. The time dependence of MD trajectories for BChE-catalyzed hydrolysis of ACh (not shown) is very similar to that of the corresponding MD trajectories depicted in Figure 2 for AChE-catalyzed hydrolysis of ACh. The time-dependence of MD trajectories for BChE-catalyzed hydrolysis of (−)-cocaine (not shown) is very similar to that of the corresponding MD trajectories depicted in Figure 3 for BChE-catalyzed hydrolysis of (+)-cocaine. The numerical results obtained for all of the MD trajectories (starting from a snapshot after the MD simulation was stabilized) are summarized in Table 1. As seen in Table 1, the RMSD values are all smaller than 2.0 Å for all of the MD trajectories, demonstrating that the backbones of the proteins did not dramatically change in going from ES to TS1 and INT1. The internuclear distances between the carbonyl oxygen of ACh/cocaine and the peptidic NH hydrogen atoms of G121/G116, G122/G117, and A204/A199 of AChE/BChE are denoted by D1, D2, and D3, respectively, in Table 1 and Figures 2 and 3.

As revealed by Figure 2 and Table 1, for AChE-catalyzed hydrolysis of ACh, the carbonyl oxygen of ACh forms N−H···O hydrogen bonds with the peptidic NH hydrogen atoms of G122 and A204 of AChE in the simulated ES structure. In going from ES to TS1 and INT1, these two N−H···O hydrogen bonds become stronger and stronger as the simulated H···O distances become shorter and shorter, while the ACh carbonyl oxygen forms another strong N−H···O hydrogen bond with the NH

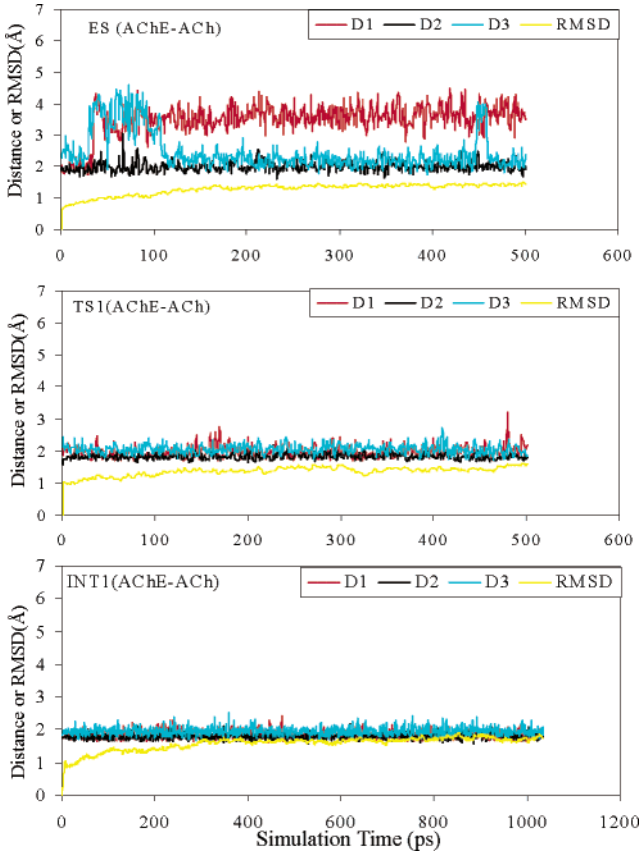

Figure 2. Plots of the key internuclear distances (in Å) versus the simulation time in the simulated ES, TS1, and INT1 structures for AChE-catalyzed hydrolysis of ACh. Traces D1, D2, and D3 refer to the distances between the carbonyl oxygen of ACh and the NH hydrogen of G121, G122, and A204, respectively. RMSD represents the root-mean-square deviation (in Å) of the simulated positions of AChE backbone atoms from those in the initial structure.

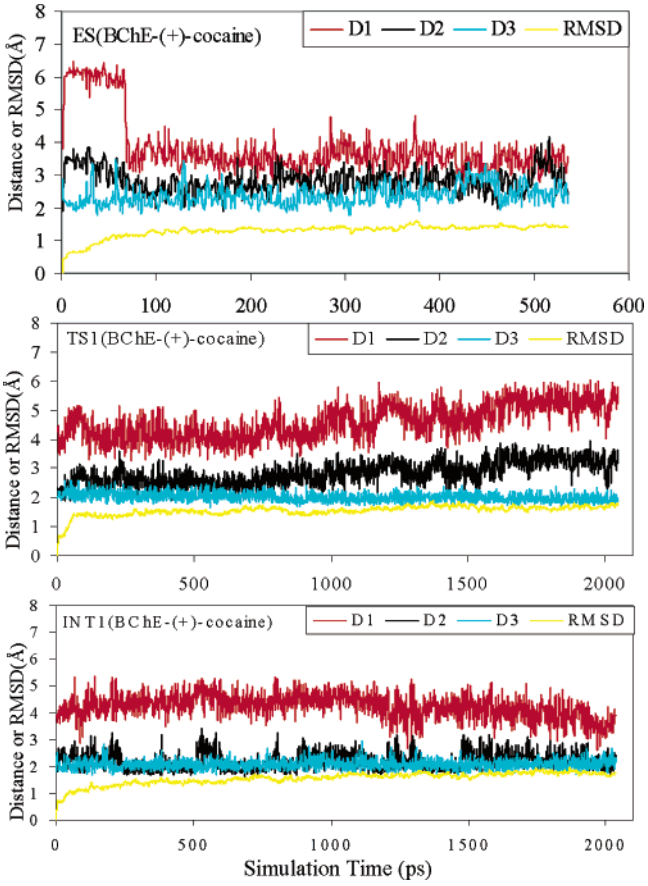

Figure 3. Plots of the key internuclear distances (in Å) versus the simulation time in the simulated ES, TS1, and INT1 structures for BChE-catalyzed hydrolysis of (+)-cocaine. Traces D1, D2, and D3 refer to the distances between the carbonyl oxygen of (+)-cocaine benzoyl ester and the NH hydrogen of G116, G117, and A199, respectively. RMSD represents the root-mean-square deviation (in Å) of the simulated positions of BChE backbone atoms from those in the initial structure.

hydrogen atom of G121. The number of N−H···O hydrogen bonds in the MD-simulated ES, TS1, and INT1 structures is in line with the previous computational results reported in the literature. McCammon et al.[27,49] reported MD simulations and QM/MM calculations on the mouse AChE−ACh system. Their MD simulations[49] were performed on the prereactive AChE−ACh complex, whereas their QM/MM calculations[27] were carried out on the initial step of the acylation stage of the AChE-catalyzed ACh hydrolysis. Their QM/MM results indicate that in the AChE−ACh Michaelis complex, two hydrogen bonds exist between the carbonyl oxygen of ACh and the peptidic NH groups of G121 and G122. In going from the AChE−ACh Michaelis complex to the transition state and intermediate, the distance between the carbonyl oxygen of ACh and the NH hydrogen of A204 becomes shorter, and the third hydrogen bond is formed both in the transition state and in the tetrahedral intermediate.[27] These results demonstrate that the QM/MM calculations and our MD simulations both can lead to qualitatively the same results concerning the enzyme−substrate hydrogen bonding during the catalyzed hydrolysis. We elected to perform MD simulations because the MD simulations provide additional dynamics information about the hydrogen bonds. As seen in Figure 2 and Table 1, the MD results show that the fluctuation of a simulated H···O distance is correlated with the simulated average H···O distance. When the three average H···O distances become shorter and shorter in going from ES to TS1 and INT1, the corresponding fluctuations of the distances become smaller and smaller.

For BChE-catalyzed hydrolysis of (+)-cocaine, the MD-simulated ES structure shows a weak N−H···O hydrogen bond between the carbonyl oxygen of the (+)-cocaine benzoyl ester and the peptidic NH hydrogen atom of A199 of BChE; the average H···O distance (D3) is ∼2.38 Å. As seen in Table 1, the average H···O distance significantly decreases to ∼2.08 Å in both TS1 and INT1. Meanwhile, the (+)-cocaine carbonyl oxygen rarely has a hydrogen bonding contact with the NH hydrogen atom of G117 of BChE in the simulated ES structure; the minimum D2 value is ∼1.89 Å, but the average D2 value is ∼2.82 Å. The average D2 value becomes ∼2.45 and ∼2.27 Å in the simulated TS1 and INT1 structures, respectively.

For BChE-catalyzed hydrolysis of (−)-cocaine, the MD-simulated ES structure shows only one N−H···O hydrogen bond between the carbonyl oxygen of the (−)-cocaine benzoyl ester and the peptidic NH hydrogen atom of G117 of BChE; the average H···O distance (D3) is ∼2.14 Å. In the MD-simulated TS1 structure, the hydrogen bonding with G117 becomes much weaker while a new N−H···O hydrogen bond forms with the peptidic NH hydrogen atom of A199. In going from TS1 to INT1, the N−H···O hydrogen bond with G117 becomes much stronger while the N−H···O hydrogen bond with A199 becomes weaker.

Comparing BChE-catalyzed hydrolysis of (−)-cocaine with BChE-catalyzed hydrolysis of (+)-cocaine, we can see that the overall strength of the hydrogen bonding of (−)-cocaine with

TABLE 1: Summary of the MD-Simulated Key Distances (Å) and the Root-Mean-Square Deviation (RMSD) of the Simulated Structures from the Corresponding Initial Structures

simulated system	type of distance	distance[a] D1	D2	D3	RMSD[b]
ES(AChE-ACh)	average	3.60	2.00	2.27	1.36
	maximum	4.48	2.55	4.06	1.50
	minimum	2.78	1.60	1.75	1.06
	fluctuation	0.32	0.15	0.36	0.08
TS1(AChE-ACh)	average	1.97	1.83	2.06	1.40
	maximum	3.21	2.21	2.74	1.61
	minimum	1.69	1.63	1.71	1.07
	fluctuation	0.18	0.09	0.15	0.10
INT1(AChE-ACh)	average	1.85	1.81	1.95	1.63
	maximum	2.43	2.17	2.52	1.90
	minimum	1.58	1.58	1.64	1.28
	fluctuation	0.12	0.09	0.12	0.13
ES(BChE-ACh)	average	3.60	2.03	2.28	1.26
	maximum	3.71	2.10	2.75	1.46
	minimum	3.49	1.96	1.82	1.06
	fluctuation	0.16	0.10	0.66	0.29
TS1(BChE-ACh)	average	1.93	1.92	2.06	1.46
	maximum	2.80	2.55	2.53	1.77
	minimum	1.61	1.61	1.67	1.15
	fluctuation	0.16	0.13	0.14	0.10
INT1(BChE-ACh)	average	1.86	1.76	1.88	1.67
	maximum	3.26	2.22	2.35	1.89
	minimum	1.60	1.57	1.60	1.40
	fluctuation	0.13	0.09	0.10	0.07
ES(BChE-(+)-cocaine)	average	3.83	2.82	2.38	1.29
	maximum	6.45	4.15	3.44	1.60
	minimum	2.70	1.89	1.77	0.00
	fluctuation	0.88	0.37	0.31	0.20
TS1(BChE-(+)-cocaine)	average	4.15	2.45	2.08	1.48
	maximum	5.00	2.95	2.47	1.54
	minimum	3.44	1.95	1.85	1.40
	fluctuation	0.35	0.24	0.14	0.03
INT1(BChE-(+)-cocaine)	average	3.93	2.27	2.08	1.75
	maximum	5.13	3.19	2.68	1.96
	minimum	2.62	1.71	1.73	1.50
	fluctuation	0.42	0.28	0.17	0.07
ES(BChE-(−)-cocaine)	average	3.79	2.14	4.47	1.28
	maximum	5.24	3.66	6.00	1.70
	minimum	2.71	1.75	2.56	0.00
	fluctuation	0.40	0.27	0.36	0.26
TS1(BChE-(−)-cocaine)	average	4.59	2.91	1.92	1.59
	maximum	5.73	4.14	2.35	1.90
	minimum	3.35	1.97	1.61	1.37
	fluctuation	0.35	0.35	0.12	0.10
INT1(BChE-(−)-cocaine)	average	3.92	1.94	2.36	1.57
	maximum	4.85	2.46	2.93	1.82
	minimum	2.70	1.65	1.81	1.35
	fluctuation	0.37	0.16	0.20	0.09

[a] D1, D2, and D3 represent the internuclear distances between the carbonyl oxygen of the substrate ACh/cocaine and the NH hydrogen of G121/G116, G122/G117, and A204/A199 of AChE/BChE, respectively. [b] Root-mean-square deviation of the coordinates of backbone atoms in the simulated structure from those in the initial structure.

the oxyanion hole of BChE should be close to that of (+)-cocaine for each type of MD-simulated structure (ES, TS1, or INT1), although the strengths of the individual N−H···O hydrogen bonds should be significantly different. The average D1, D2, and D3 values summarized in Table 1 reveal that the overall strength of the hydrogen bonding of (−)-cocaine with the oxyanion hole of BChE should be slightly weaker than that of (+)-cocaine in the TS1 and INT1 structures. Comparing BChE-catalyzed hydrolysis of (+)/(−)-cocaine with AChE-catalyzed hydrolysis of ACh, a remarkable difference is that G116 of BChE does not form a hydrogen bond with (+)/(−)-cocaine, whereas the corresponding residue G121 of AChE forms a strong N−H···O hydrogen bond with ACh in the simulated TS1 and INT1 structures. This remarkable difference is likely due to the different sizes of the leaving group in the substrate hydrolysis. The leaving group in cocaine is a substituted tropane ring, whereas the size of the leaving group, i.e., $OCH_2CH_2N^+(CH_3)_3$, in ACh is much smaller. The formation of the possible hydrogen bond between the backbone NH of G116 and the carbonyl oxygen of cocaine is apparently hindered by the tropane ring of cocaine. To examine this issue, we also performed MD simulations on the ES, TS1, and INT1 structures for BChE-catalyzed hydrolysis of ACh. As seen in Table 1, the simulated H···O distances of the N−H···O hydrogen bonds in the ES, TS1, and INT1 structures for BChE-catalyzed hydrolysis of ACh are very similar to the corresponding H···O distances in the simulated ES, TS1, and INT1 structures for AChE-catalyzed hydrolysis of ACh. These results clearly indicate that the remarkable hydrogen bonding difference between AChE-catalyzed hydrolysis of ACh and BChE-catalyzed hydrolysis of (+)/(−)-cocaine is indeed due to the significantly different sizes of the leaving group in the substrate hydrolysis.

It should be pointed out that for BChE-catalyzed hydrolysis of (+)/(−)-cocaine, the initial structure used in the final, fully relaxed MD simulation of the TS1 (or INT1) structure did not have a hydrogen bond between G116 and cocaine; the initial structure was constructed from the corresponding MD-simulated ES structure by performing energy minimization and equilibration. We wanted to know whether different initial structures used in the MD simulations would lead to dramatically different results or not concerning the hydrogen bonding in the TS1 (or INT1) structure for BChE-catalyzed cocaine hydrolysis. In a particular test on the TS1 structure for BChE-catalyzed hydrolysis of (−)-cocaine, the initial TS1 structure used in the MD simulation was still constructed from the MD-simulated ES structure by energy minimization, but we first used a constraint on each of the three H···O distances (D1 to D3) between the carbonyl oxygen of (−)-cocaine and the NH hydrogen of G116, G117, and A199. The three H···O distances (D1 to D3) were all constrained to 2.0 Å. The constrained MD simulation quickly led to three N−H···O hydrogen bonds between the carbonyl oxygen of (−)-cocaine and the backbone NH of G116, G117, and A199 and the constrained MD simulation was continued for 500 ps. The TS1 structure obtained from the constrained MD simulation was then used as the new initial structure to perform the fully relaxed MD simulation. It turned out that during the fully relaxed MD simulation, the NH hydrogen of G116 quickly left the carbonyl oxygen of (−)-cocaine, while the H···O distance (D2) between the carbonyl oxygen of (−)-cocaine and the NH hydrogen of G117 also became ∼1.0 Å longer than the constrained 2.0 Å. The final D1, D2, and D3 values obtained in this way were qualitatively consistent with the corresponding D1, D2, and D3 values summarized in Table 1, suggesting that the outcome of the MD simulation on the TS1 structure was not very sensitive to the initial TS1 geometry used in the fully relaxed MD simulation.

Hydrogen Bonding Energies. With each of the simulated H···O distances, we estimated the hydrogen bonding energy (HBE) by using the general HBE equation implemented in the AutoDock 3.0 program suite.[50] Specifically, for each N−H···O hydrogen bond with the substrate carbonyl oxygen, a HBE value can be evaluated with each snapshot of the MD-simulated structure. The final HBE of an MD-simulated hydrogen bond was evaluated as the average HBE value of all snapshots taken from the stable MD trajectory. Table 2 shows the total hydrogen

TABLE 2: Calculated Total Hydrogen Bonding Energies (HBE in kcal/mol) in the Simulated ES, TS1, and INT1 Structures for AChE-Catalyzed Hydrolysis of ACh, BChE-Catalyzed Hydrolysis of ACh, BChE-Catalyzed Hydrolysis of (+)-Cocaine, and BChE-Catalyzed Hydrolysis of (−)-Cocaine

				ΔHBE	
	ES	TS1	INT1	ES→TS1[a]	TS1→INT1[b]
AChE-ACh	−6.5	−11.9	−12.5	−5.4	−0.6
BChE-ACh	−6.5	−10.9	−15.7	−4.4	−4.8
BChE-(+)-cocaine	−2.7	−4.4	−6.3	−1.7	−1.9
BChE-(−)-cocaine	−3.4	−4.2	−5.3	−0.8	−0.9

[a] Change of the total hydrogen bonding energy from ES to TS1, i.e., ΔHBE(ES→TS1) = HBE(TS1) − HBE(ES). [b] Change of the total hydrogen bonding energy from TS1 to INT1, i.e., ΔHBE(TS1→INT1) = HBE(INT1) − HBE(TS1).

bonding energy for all of the hydrogen bonds between the substrate carbonyl oxygen and the oxyanion hole for each of the MD-simulated structures.

As seen in Table 2, the calculated total hydrogen bonding affinity generally increases in going from ES to TS1 and to INT1 for each of the four MD-simulated reaction systems. This means that the overall hydrogen bonding between the substrate carbonyl oxygen and the oxyanion hole always favors the stabilization of the transition state (TS1) relative to the ES structure for these enzymatic reactions. The change of the total HBE from ES to TS1, i.e., ΔHBE(ES→TS1) = HBE(TS1) − HBE(ES), approximately reflects the energetic contribution of the overall hydrogen bonding between the substrate carbonyl oxygen and the oxyanion hole to the stabilization of transition state TS1 and to the lowering of the corresponding energy barrier. The calculated ΔHBE(ES→TS1) values are −5.4, −4.4, −1.7, and −0.8 kcal/mol for AChE-catalyzed hydrolysis of ACh, BChE-catalyzed hydrolysis of ACh, BChE-catalyzed hydrolysis of (+)-cocaine, and BChE-catalyzed hydrolysis of (−)-cocaine, respectively. These ΔHBE(ES→TS1) values suggest that the oxyanion hole of AChE or BChE may lower the energy barrier of the ACh hydrolysis by ∼5.4 or ∼4.4 kcal/mol, whereas the oxyanion hole of BChE may only lower the energy barrier of the (+)- or (−)-cocaine hydrolysis by ∼1.7 or ∼0.8 kcal/mol. The difference of about 3 to 5 kcal/mol in the ΔHBE(ES→TS1) value between the ACh hydrolysis and the cocaine hydrolysis is certainly not the only factor affecting the energy barrier, but it helps to qualitatively understand the experimental fact that the catalytic activity of AChE against ACh is considerably higher than that of BChE against cocaine.[1,6] This implies that the catalytic activity of BChE against cocaine could be improved by enhancing the hydrogen bonding between the cocaine carbonyl oxygen and the oxyanion hole of BChE, particularly in the transition state, through certain mutations on some amino acid residues surrounding the oxyanion hole.

Conclusions

Molecular dynamics (MD) simulations and hydrogen bonding energy (HBE) calculations performed on the prereactive enzyme−substrate complex (ES), transition state (TS1), and intermediate (INT1) for AChE/BChE-catalyzed hydrolysis of ACh/cocaine provide some new physical insights into the hydrogen bonding of the substrate with the oxyanion hole of AChE/BChE and its role in stabilizing the transition state. Although the fundamental reaction pathway for BChE-catalyzed hydrolysis of cocaine is similar to that for AChE-catalyzed hydrolysis of ACh in terms of the breaking and formation of covalent bonds during the catalytic hydrolysis, the hydrogen bonding of cocaine with the oxyanion hole of BChE is found to be remarkably different from that of ACh with AChE/BChE. Residues G116, G117, and A199 of BChE were expected to form a three-pronged oxyanion hole like G121, G122, and A204 of AChE to stabilize the transition state for both ACh and cocaine hydrolysis. However, whereas G121/G116, G122/G117, and A204/A199 of AChE/BChE all can form N−H···O hydrogen bonds with the carbonyl oxygen of ACh to stabilize the transition state during the ACh hydrolysis, BChE only uses G117 and A199 to form relatively weaker N−H···O hydrogen bonds with the carbonyl oxygen of cocaine benzoyl ester. G116 of BChE does not form a hydrogen bond with cocaine in any of the simulated structures, whereas G121/G116 of AChE/BChE forms a strong N−H···O hydrogen bond with ACh in the simulated TS1 and INT1 structures. As a result, the calculated overall strength of the hydrogen bonding during AChE/BChE-catalyzed hydrolysis of ACh is always stronger than that during BChE-catalyzed hydrolysis of cocaine for each type of simulated structure (ES, TS1, or INT1).

The changes of the calculated total hydrogen bonding energy (HBE) from ES to TS1 are about −5.4 or −4.4 kcal/mol for AChE- or BChE-catalyzed hydrolysis of ACh and about −1.7 or −0.8 kcal/mol for BChE-catalyzed hydrolysis of (+)- or (−)-cocaine. These energetic results suggest that the oxyanion hole of AChE or BChE may lower the energy barrier of the ACh hydrolysis by about 5.4 or 4.4 kcal/mol, whereas the oxyanion hole of BChE may only lower the energy barriers of the (+)- or (−)-cocaine hydrolysis by about 1.7 or 0.8 kcal/mol. The remarkable difference of about 3 to 5 kcal/mol helps us to understand why the catalytic activity of AChE against ACh is considerably higher than that of BChE against cocaine, which provides valuable clues on how to improve the catalytic activity of BChE against cocaine.

Acknowledgment. The research was supported by NIH/NIDA (grant R01DA013930 to C.-G. Zhan). The authors also acknowledge the Center for Computational Sciences (CCS) at University of Kentucky for supercomputing time on Superdome (a shared-memory supercomputer, with 4 nodes and 256 processors).

References and Notes

(1) Quin, D. M. *Chem. Rev.* **1987**, *87*, 955−979.
(2) Darvesh, S. D.; Hopkins, A.; Geula, C. *Nat. Rev. Neurosci*. **2003**, *4*, 131−138.
(3) Mizutani, M. Y.; Itai, A. *J. Med. Chem.* **2004**, *47*, 4818−4828.
(4) Foldi, N. S.; White, R. E. C.; Schaefer, L. A. *Int. J. Geriatr. Psychiatry* **2005**, *20*, 485−488.
(5) Araujo, J. A.; Studzinski, C. M.; Milgram, N. W. *Prog. Neuro-Psychopharmacol. Biol. Psychiatry* **2005**, *29*, 411−422.
(6) Giacobini, E. editor. *Butyrylcholinesterase*: *Its Function and Inhibitors*; Dunitz Martin Ltd.: London, UK, 2003.
(7) (a) Gawin, F. H.; Ellinwood, E. H., Jr. *N. Engl. J. Med*. **1988**, *318*, 1173−1182. (b) Landry, D. W. *Sci. Am.* **1997**, *276*, 42−45.
(8) Singh, S. *Chem. Rev*. **2000**, *100*, 925−1024.
(9) Sparenborg, S.; Vocci, F.; Zukin, S. *Drug Alcohol Depend*. **1997**, *48*, 149−151.
(10) Gorelick, D. A. *Drug Alcohol Depen*. **1997**, *48*, 159−165.
(11) Browne, S. P.; Slaughter, E. A.; Couch, R. A.; Rudnic, E. M.; McLean, A. M. *Biopharm. Drug Dispos.* **1998**, *19*, 309−314.
(12) (a) Carmona, G. N.; Baum, I.; Schindler, C. W.; Goldberg, S. R.; Jufer, R. *Life Sci.* **1996**, *59*, 939−943. (b) Lynch, T. J.; Mattes, C. E.; Singh, A.; Bradley, R. M.; Brady, R. O.; Dretchen, K. L. *Toxicol. Appl. Pharmacol*. **1997**, *145*, 363−371.
(13) Mattes, C. E.; Lynch, T. J.; Singh, A.; Bradley, R. M.; Kellaris, P. A.; Brady, R. O.; Dretchen, K. L. *Toxicol. Appl. Pharmacol*. **1997**, *145*, 372−380.
(14) Mattes, C. E.; Belendiuk, G. W.; Lynch, T. J.; Brady, R. O.; Dretchen, K. L. *Addict. Biol*. **1998**, *3*, 171−188.
(15) Gateley, S. J. *Biochem. Pharmacol*. **1991**, *41*, 1249−1254.

(16) Gatley, S. J.; MacGregor, R. R.; Fowler, J. S.; Wolf, A. P.; Dewey, S. L.; Schlyer. D. J. *J. Neurochem.* **1990**, *54*, 720−723.

(17) Sussman, J. L.; Harel, M.; Frolow, F.; Oefner, C.; Goldman, A.; Toker, L.; Silman, I. *Science* **1991**, *253*, 872−879.

(18) Gilson, M. K.; Straatsma, T. P.; Mccammon, J. A.; Ripoll, D. R.; Faerman, C. H.; Axelsen, P. H.; Silman, I.; Sussman, J. L. Open back door in a molecular-dynamics simulation of acetylcholinesterase. *Science* **1994**, *263*, 1276−1278.

(19) Antosiewicz, J.; Wlodek, S. T.; McCammon, J. A. *Biopolymers* **1996**, *39*, 85−94.

(20) Zhou, H. X.; Briggs, J. M.; McCammon, J. A. *J. Am. Chem. Soc.* **1996**, *118*, 13069−13070.

(21) Wlodek, S. T.; Antosiewicz, J.; Briggs, J. M. *J. Am. Chem. Soc.* **1997**, *119*, 8159−8165.

(22) Fuxreiter, M.; Warshel, A. *J. Am. Chem. Soc.* **1998**, *120*, 183−194.

(23) Bartolucci, C.; Perola, E.; Cellai, L.; Brufani, M.; Lamba, D. *Biochemistry* **1999**, *38*, 5714−5719.

(24) Wang, Q. M.; Jiang, H. L.; Chen, K. X.; Ji, R. Y.; Ye, Y. J. *Int. J. Quantum Chem.* **1999**, *74*, 315−325.

(25) Tara, S.; Helms, V.; Straatsma, T. P.; McCammon, J. A. *Biopolymers* **1999**, *50*, 347−359.

(26) Kua, J.; Zhang, Y. K.; McCammon, J. A. *J. Am. Chem. Soc.* **2002**, *124*, 8260−8267.

(27) Zhang, Y.; Kua, J.; McCammon, J. A. *J. Am. Chem. Soc.* **2002**, *124*, 10572−10577.

(28) Kua, J.; Zhang, Y. K.; Eslami, A. C.; Butler, J. R.; McCammon, J. A. *Protein Sci.* **2003**, *12*, 2675−2684.

(29) Manojkumar, T. K.; Cui, C. Z.; Kim, K. S. *J. Comput. Chem.* **2005**, *26*, 606−611.

(30) Zhang, D. Q.; Suen, J.; Zhang, Y. J.; Song, Y. H.; Radic, Z.; Taylor, P.; Holst, M.; Bajaj, C.; Baker, N. A.; McCammon, J. A. *Biophys. J.* **2005**, *88*, 182A−182A.

(31) Zhang, D. Q.; Suen, J.; Zhang, Y. J.; Song, Y. H.; Radic, Z.; Taylor, P.; Holst, M.; Bajaj, C.; Baker, N. A.; McCammon, J. A. *Biophys. J.* **2005**, *88*, 1659−1665.

(32) (a) Masson, P.; Legrand, P.; Bartels, C. F.; Froment, M.-T.; Schopfer, L. M.; Lockridge, O. *Biochemistry* **1997**, *36*, 2266−2277. (b) Masson, P.; Xie, W.; Froment, M. T.; Levitsky, V.; Fortier, P. L.; Albaret, C.; Lockridge, O. *Biochim. Biophys. Acta* **1999**, *1433*, 281−293. (c) Xie, W.; Altamirano, C. V.; Bartels, C. F.; Speirs, R. J.; Cashman, J. R.; Lockridge, O. *Mol. Pharmacol.* **1999**, *55*, 83−91. (d) Duysen, E. G.; Bartels, C. F.; Lockridge, O. *J. Pharmacol. Exp. Ther.* **2002**, *302*, 751−758. (e) Nachon, F.; Nicolet, Y.; Viguie, N.; Masson, P.; Fontecilla-Camps, J. C.; Lockridge, O. *Eur. J. Biochem.* **2002**, *269*, 630−637. (f) Zhan, C.-G.; Landry, D. W. *J. Phys. Chem. A* **2001**, *105*, 1296−1301.

(33) Berkman, C. E.; Underiner, G. E.; Cashman, J. R. *Biochem. Pharmcol.* **1997**, *54*, 1261−1266.

(34) (a) Sun, H.; El Yazal, J.; Lockridge, O.; Schopfer, L. M.; Brimijoin, S.; Pang, Y. P. *J. Biol. Chem.* **2001**, *276*, 9330−9336. (b) Sun, H.; Shen, M. L.; Pang, Y. P.; Lockridge, O.; Brimijoin, S. *J. Pharmacol. Exp. Ther.* **2002**, *302*, 710−716. (c) Sun, H.; Pang, Y. P.; Lockridge, O.; Brimijoin, S. *Mol. Pharmacol.* **2002**, *62*, 220−224.

(35) Zhan, C.-G.; Zheng, F.; Landry, D. W. *J. Am. Chem. Soc.* **2003**, *125*, 2462−2474.

(36) Hamza, A.; Cho, H.; Tai, H.-H.; Zhan, C.-G. *J. Phys. Chem. B* **2005**, *109*, 4776−4782.

(37) Kryger, G.; Harel, M.; Giles, K.; Toker, L.; Velan, B.; Lazar, A.; Kronman, C.; Barak, D.; Ariel, N.; Shafferman, A.; Silman, I.; Sussman, J. L. *Acta Crystallogr., Sect. D* **2000**, *56*, 1385−1394.

(38) (a) Bernstein, F. C.; Koetzle, T. F.; Williams, G. J.; Meyer, E. F.; Brice, M. D.; Rodgers, J. R.; Kennard, O.; Shimanouchi, T.; Tasumi, M. *J. Mol. Biol.* **1977**, *112*, 535−542. (b) http://www.rcsb.org/pdb/.

(39) Nicolet, Y.; Lockridge, O.; Masson, P.; Fontecilla-Camps, J. C.; Nachon, F. *J. Biol. Chem.* **2003**, *278*, 41141−41147.

(40) Sali, A.; Blundell, T. L. *J. Mol. Biol.* **1990**, *212*, 403−208.

(41) Sali, A.; Blundell, T. L. *J. Mol. Biol.* **1993**, *234*, 779−815.

(42) Case, D. A.; Pearlman, D. A.; Caldwell, J. W.; Cheatham, T. E., III; Wang, J.; Ross, W. S.; Simmerling, C. L.; Darden, T. A.; Merz, K. M.; Stanton, R. V.; Cheng, A. L.; Vincent, J. J.; Crowley, M.; Tsui, V.; Gohlke, H.; Radmer, R. J.; Duan, Y.; Pitera, J.; Massova, I.; Seibel, G. L.; Singh, U. C.; Weiner, P. K.; Kollman, P. A. *AMBER 7*; University of California: San Francisco, CA, 2002.

(43) Frisch, M. J.; Trucks, G. W.; Schlegel, H. B.; Scuseria, G. E.; Robb, M. A.; Cheeseman, J. R.; Montgomery, J. A., Jr.; Vreven, T.; Kudin, K. N.; Burant, J. C.; Millam, J. M.; Iyengar, S. S.; Tomasi, J.; Barone, V.; Mennucci, B.; Cossi, M.; Scalmani, G.; Rega, N.; Petersson, G. A.; Nakatsuji, H.; Hada, M.; Ehara, M.; Toyota, K.; Fukuda, R.; Hasegawa, J.; Ishida, M.; Nakajima, T.; Honda, Y.; Kitao, O.; Nakai, H.; Klene, M.; Li, X.; Knox, J. E.; Hratchian, H. P.; Cross, J. B.; Adamo, C.; Jaramillo, J.; Gomperts, R.; Stratmann, R. E.; Yazyev, O.; Austin, A. J.; Cammi, R.; Pomelli, C.; Ochterski, J. W.; Ayala, P. Y.; Morokuma, K.; Voth, G. A.; Salvador, P.; Dannenberg, J. J.; Zakrzewski, V. G.; Dapprich, S.; Daniels, A. D.; Strain, M. C.; Farkas, O.; Malick, D. K.; Rabuck, A. D.; Raghavachari, K.; Foresman, J. B.; Ortiz, J. V.; Cui, Q.; Baboul, A. G.; Clifford, S.; Cioslowski, J.; Stefanov, B. B.; Liu, G.; Liashenko, A.; Piskorz, P.; Komaromi, I.; Martin, R. L.; Fox, D. J.; Keith, T.; Al-Laham, M. A.; Peng, C. Y.; Nanayakkara, A.; Challacombe, M.; Gill, P. M. W.; Johnson, B.; Chen, W.; Wong, M. W.; Gonzalez, C.; Pople, J. A. *Gaussian 03*, Revision A.1; Gaussian, Inc.: Pittsburgh, PA, 2003.

(44) Jorgensen, W. L.; Chandrasekhar, J.; Madura, J. D.; Klein, M. L. *J. Chem. Phys.* **1983**, *79*, 926−935.

(45) (a) Zhan, C.-G.; Norberto de Souza, O.; Rittenhouse, R.; Ornstein, R. L. *J. Am. Chem. Soc.* **1999**, *121*, 7279−7282. (b) Koca, J.; Zhan, C.-G.; Rittenhouse, R.; Ornstein, R. L. *J. Am. Chem. Soc.* **2001**, *123*, 817−826. (c) Koca, J.; Zhan, C.-G.; Rittenhouse, R. C.; Orstein, R. L. *J. Comput. Chem.* **2003**, *24*, 368−378. (d) Hamza, A.; Cho, H.; Tai, H.-H.; Zhan, C.-G. *Bioorg. Med. Chem.* **2005**, *13/14*, 4544−4551.

(46) Berendsen, H. J. C.; Postma, J. P. M.; van Gunsteren, W. F.; DiNola, A.; Haak, J. R. *J. Chem. Phys.* **1984**, *81*, 3684−3690.

(47) Ryckaert, J. P.; Ciccotti, G.; Berendsen, H. J. C. *J. Comput. Phys.* **1977**, *23*, 7−341.

(48) Darden, T. A.; Lee, H.; Pedersen, L. G. *J. Chem. Phys.* **1993**, *98*, 10089−10092.

(49) Tai, K.; Shen, T.; Börjesson, U.; Philippopoulos, M.; McCammo, J. A. *Biophys. J.* **2001**, *81*, 715−724.

(50) (a) Morris, G. M.; Goodsell, D. S.; Halliday, R. S.; Huey, R.; Hart, W. E.; Belew, R. K.; Olson, A. J. *J. Comput. Chem.* **1998**, *19*, 1639−1662. (b) Based on the general HBE equation, we have $\mathrm{HBE}(r) \approx 5\epsilon r_0^{12}/r^{12} - 6\epsilon r_0^{10}/r^{10}$, in which r is the H···O distance in the considered hydrogen bond and $\mathrm{HBE}(r) = -5.0$ kcal/mol when $r = 1.90$ Å.